

Supporting Information for

An inducible hACE2 transgenic mouse model recapitulates SARS-CoV-2 infection and pathogenesis *in vivo*

Kuo Liu, Muxue Tang, Wei Xu, Xinfeng Meng, Hengwei Jin, Maoying Han, Jing Pu, Yutang Li, Fanke Jiao, Ruilin Sun, Ruling Shen, Kathy O. Lui, Lu Lu*, Bin Zhou*

*Corresponding authors: Lu Lu, Bin Zhou.

Email: lul@fudan.edu.cn (L.L.), zhoubin@sibs.ac.cn (B.Z.)

This PDF file includes:

Figures S1 to S4

Fig. S1.

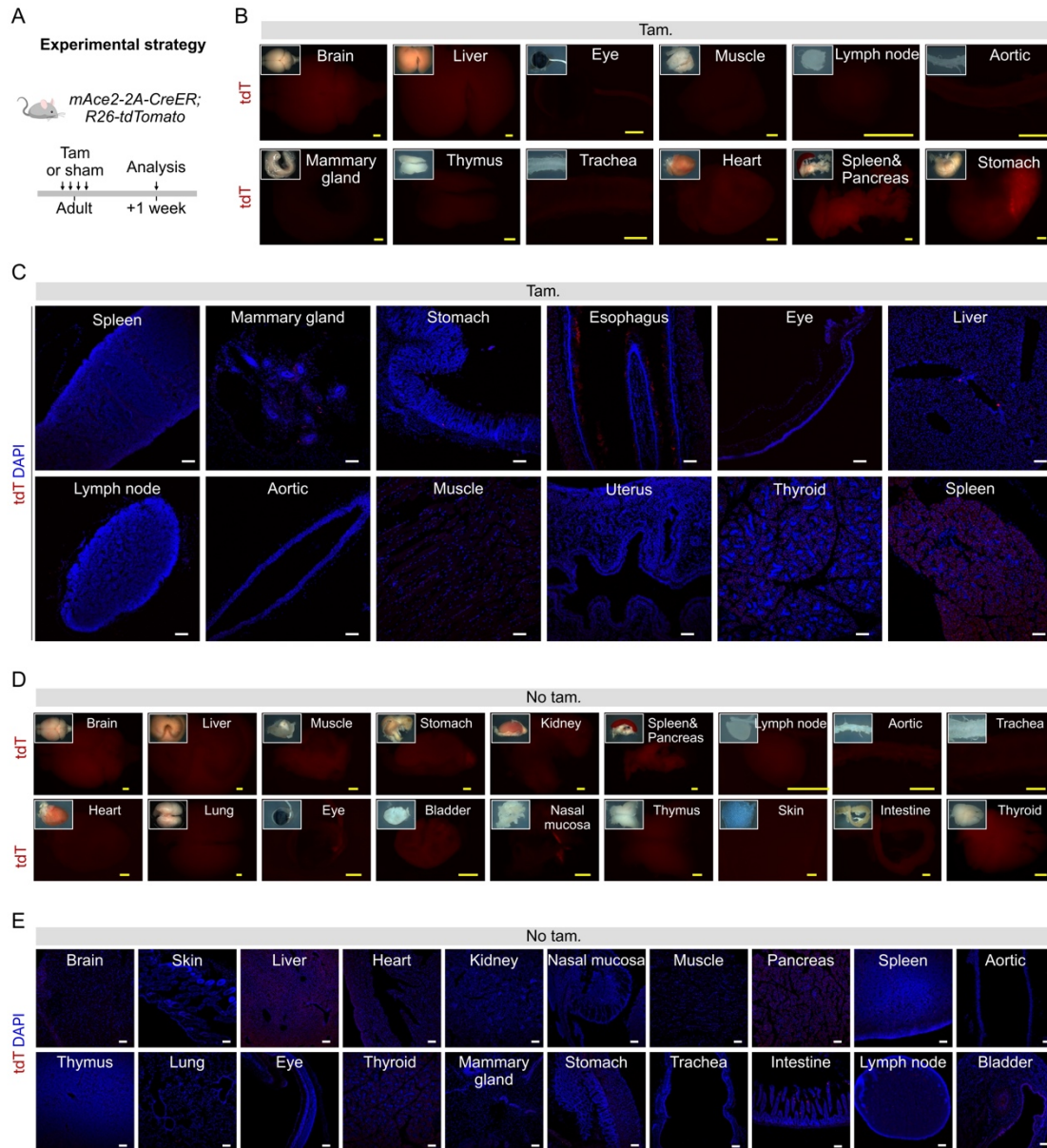


Figure S1

Fig. S1. Generation and characterization of *mAce2-2A-CreER* line. (A) A schematic diagram illustrating the experimental design. (B) Whole-mount fluorescent images of organs of *mAce2-2A-CreER;R26-tdTomato* mice after tamoxifen induction. (C) Immunostaining for tdTomato on tissue sections after tamoxifen treatment. (D) Whole-mount fluorescent images of organs without tamoxifen treatment. (E) immunostaining for tdTomato on tissue sections without tamoxifen treatment. Scale bars, yellow, 1 mm; white, 100 μ m.

Fig. S2.

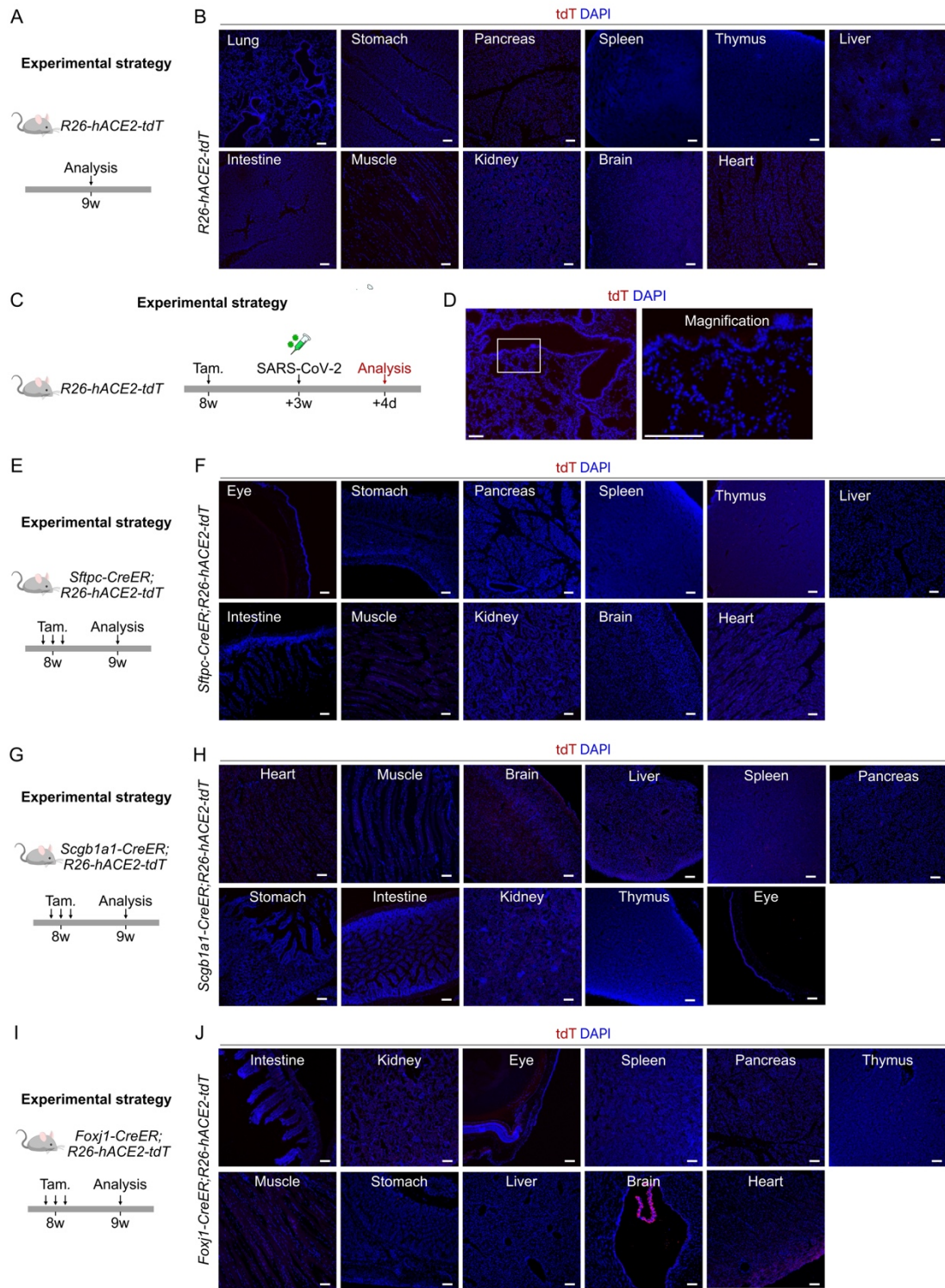


Figure S2

Fig. S2. Characterization of *R26-hACE2-tdT* line. (A and B) A schematic diagram illustrating the experimental design (A) and immunostaining for tdTomato on tissues sections of *R26-hACE2-tdT*

mice (B). (C) A schematic diagram illustrating the virus infection strategy. (D) Immunostaining for tdT on infected lung sections of *R26-hACE2-tdT*. (E and F) A schematic diagram illustrating the experimental design (E) and immunostaining for tdTomato on tissues sections of *Sftpc-CreER;R26-hACE2-tdT* mice after tamoxifen treatment (F). (G and H) A schematic diagram illustrating the experimental design (G) and immunostaining for tdTomato on tissues sections of *Scgb1a1-CreER;R26-hACE2-tdT* mice after tamoxifen treatment (H). (I and J) A schematic diagram illustrating the experimental design (I) and immunostaining for tdTomato on tissues sections of *Foxj1-CreER;R26-hACE2-tdT* mice after tamoxifen treatment (J). Scale bars, 100 μ m.

Fig. S3.

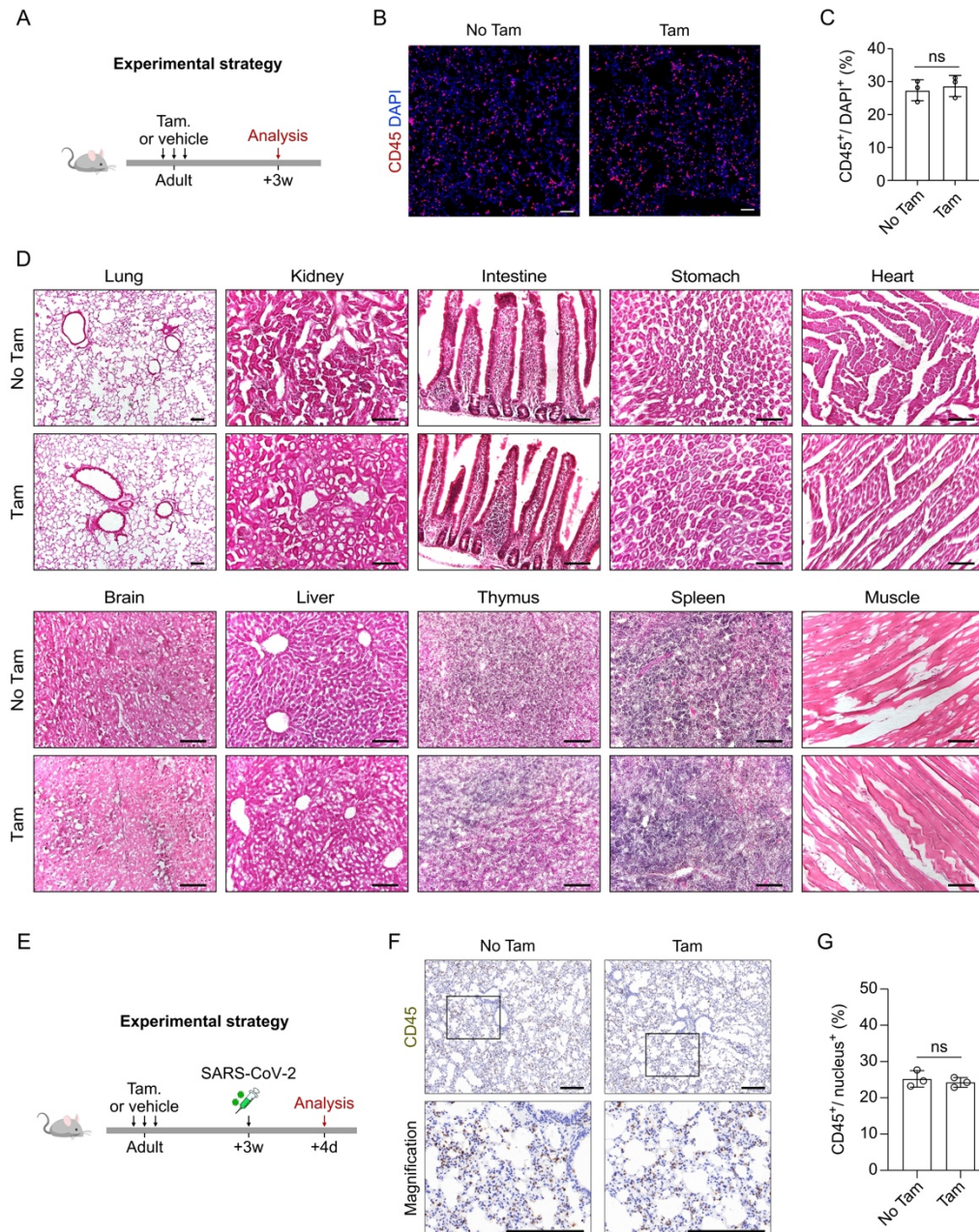


Figure S3

Fig. S3. No significant toxicity and immune effects were induced by tamoxifen treatment. (A) A schematic diagram illustrating the experimental strategy. The lungs were collected 3 weeks post tamoxifen or corn oil (vehicle) treatment. (B) Immunostaining for CD45 on lung sections in (A). (C) Quantification of percentage of CD45⁺ cells in DAPI⁺ cells in (B). *P* value was calculated by unpaired two-tailed Student's *t*-test. ns, no significance. Data are the mean \pm SD; *n* = 3. (D) H&E staining of the tissues sections post 3 weeks tamoxifen or corn oil (vehicle) treatment. (E) A

schematic diagram illustrating the experimental strategy. (F) IHC staining for CD45⁺ immune cells on lung sections in (E). (G) Quantification of percentage of CD45⁺ cells in nucleus⁺ cells in (F). *P* value was calculated by unpaired two-tailed Student's *t*-test. ns, no significance. Data are the mean \pm SD; n = 3. Scale bars, white, 100 μ m. black, 200 μ m.

Fig. S4.

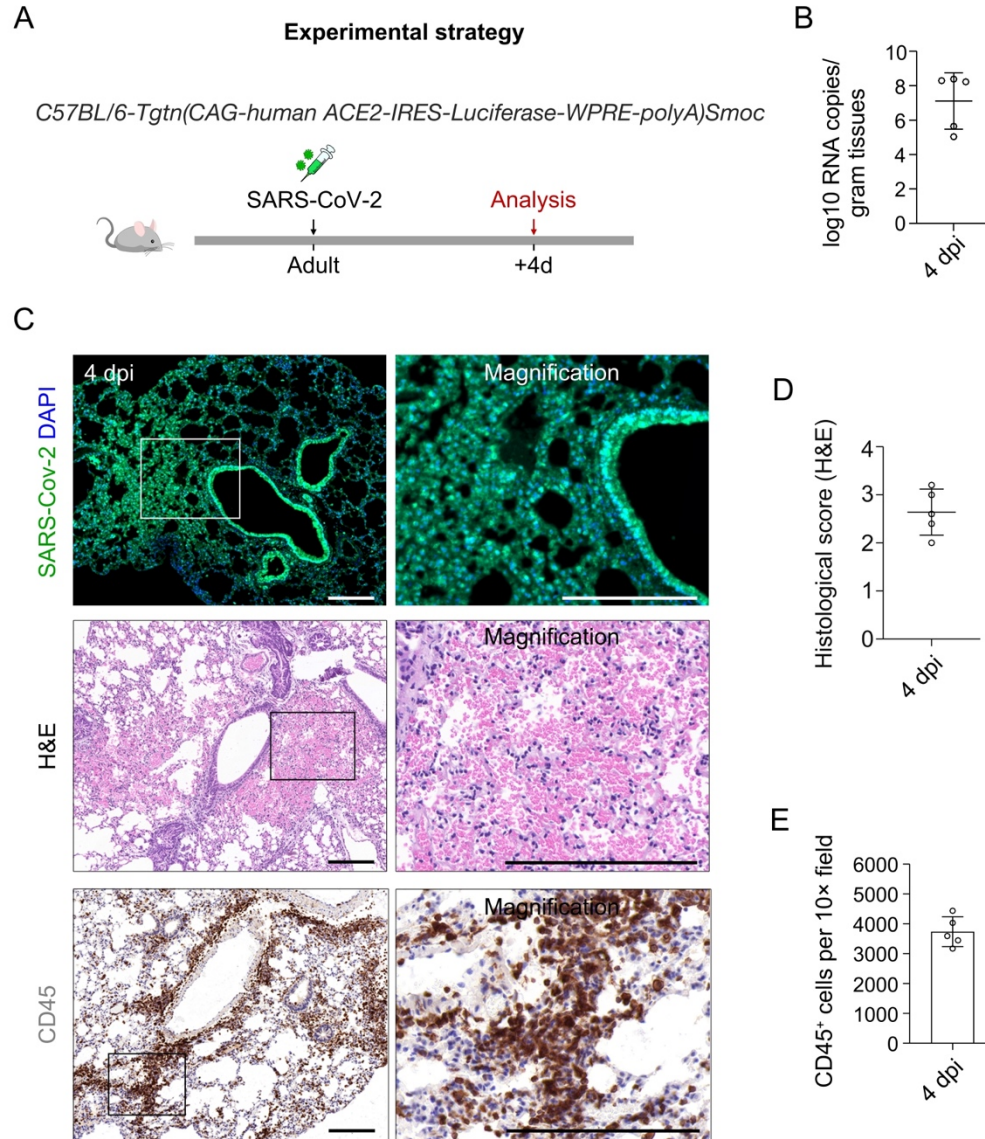


Figure S4

Fig. S4. Pathological changes on a CAG promoter driven hACE2 mice after SARS-CoV-2 infection. (A) A schematic diagram illustrating the experimental design. (B) RTq-PCR quantification of SARS-CoV-2 ORF gene expression in the lungs at 4 dpi. Data are presented as mean \pm SD; n = 5 mice per group. (C) Immunostaining for SARS-CoV-2 S protein on lung sections at 4 dpi (up panel). H&E staining of the infected lung tissues at 4 dpi (middle panel). IHC staining for CD45 on lung sections at 4 dpi (down panel). (D) H&E score of the lung injuries at at 4 dpi. N = 5 mice per group. (E) Quantification the cell number of CD45⁺ immune cells of infected lung tissues. Data are presented as mean \pm SD; n = 5 mice per group. Scale bars, white, 100 μ m; black, 200 μ m.